

Redox- and pH-Responsive Orthogonal Supramolecular Self-Assembly: An Ensemble Displaying Molecular Switching Characteristics

Dong Sub Kim,[†] Jinho Chang,^{*,†,§} Soojung Leem,[†] Jung Su Park,^{||} Pall Thordarson,^{*,‡} and Jonathan L. Sessler^{*,†}

[†]Department of Chemistry, The University of Texas at Austin, 105 East 24th Street, Stop A5300, Austin, Texas 78712-1224, United States

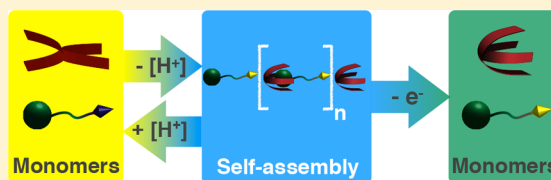
[§]Department of Chemistry, Sungshin Women's University, 55 Dobong-ro, 76 ga-gil, Gangbuk-gu, Seoul 142-732, Republic of Korea

^{||}Department of Chemistry, Sookmyung Women's University, Seoul 140-742, Korea

[‡]School of Chemistry, The University of New South Wales, Sydney, New South Wales 2052, Australia

Supporting Information

ABSTRACT: Two heteroditopic monomers, namely a thiopropyl-functionalized tetrathiafulvalene-annulated calix[4]pyrrole (SPr-TTF-C[4]P **1**) and phenyl C₆₁ butyric acid (PCBA **2**), have been used to assemble a chemically and electrochemically responsive supramolecular ensemble. Addition of an organic base initiates self-assembly of the monomers via a molecular switching event. This results in the formation of materials that may be disaggregated via the addition of an organic acid or electrolysis.



INTRODUCTION

Precise control of complex chemical systems through the application of an external stimulus continues to attract interest due to potential applications in the area of functional and adaptive smart materials, including drug delivery systems^{1–5} and self-healing materials.^{6–9} Supramolecular approaches, which exploit the reversible nature of noncovalent interactions, have proved especially useful in the construction of self-assembled and responsive materials. Systems that respond to light,^{10,11} heat,^{12,13} ions, or small molecules^{14–18} are now known. Of particular interest are materials that rely on so-called “orthogonal” interactions,¹⁹ e.g., a combination of hydrogen-bonding interactions and metal–ligand interactions, since this typically provides greater predictability in the context of self-assembly as well as a larger number of stimuli that may be used to control the system.

While there are quite a few examples of self-assembled materials created via orthogonal noncovalent interactions,^{20,21} oligomeric constructs built up from heteroditopic monomers that themselves display stimuli-responsive, molecular switching behavior have yet to be reported. Such constructs may allow for a level of stimulus-based control that is not otherwise possible. Herein, we report a redox- and pH-responsive self-assembled system built up from two discrete heteroditopic monomers, namely a thiopropyl-functionalized tetrathiafulvalene-annulated calix[4]pyrrole (SPr-TTF-C[4]P **1**) and phenyl C₆₁ butyric acid²² (PCBA **2**). Self-assembly of these monomers is initiated via the conformational switching of **1** by simple acid and base

chemistry; the system may be further regulated through electrochemical and pH effects.

Recently, Fukuzumi and Sessler found that anion-bound tetrathiafulvalene-annulated calix[4]pyrroles (TTF-C[4]Ps) are able to form 1:1 complexes with C₆₀, Li@C₆₀, or C₇₀, wherein the fullerene is bound within their bowl-like pockets of the calix[4]pyrroles via charge-transfer (CT) interaction both in solution and the solid state.^{23,24} These complexes are not formed in the absence of anions, and their stability is greatly reduced in the presence of competitive guests, such as the tetraethylammonium cation. In general, in the absence of a coordinating anion, calix[4]pyrroles (C[4]Ps) adopt the thermodynamically more stable, 1,3-alternate conformation in noncompetitive solvents. However, in the presence of a coordinating anion, C[4]Ps are converted to the corresponding anion-bound cone-like conformers.²⁵ The fullerene-TTF-C[4]P complexes are thus the product of a specific molecular switching process, wherein an anion salt containing a noncompetitive counterion is used to create the form suitable for, e.g., C₆₀ binding. This degree of control led us to consider that TTF-C[4]Ps, if paired with a suitably anion-functionalized fullerene, could be used to create a new class of stimulus responsive materials whose function could be controlled at the monomer level via conformational switching.

To test the above hypothesis, we chose to use SPr-TTF-C[4]P (**1**) in conjunction with phenyl C₆₁ butyric acid (PCBA **2**),

Received: June 30, 2015

Published: November 25, 2015

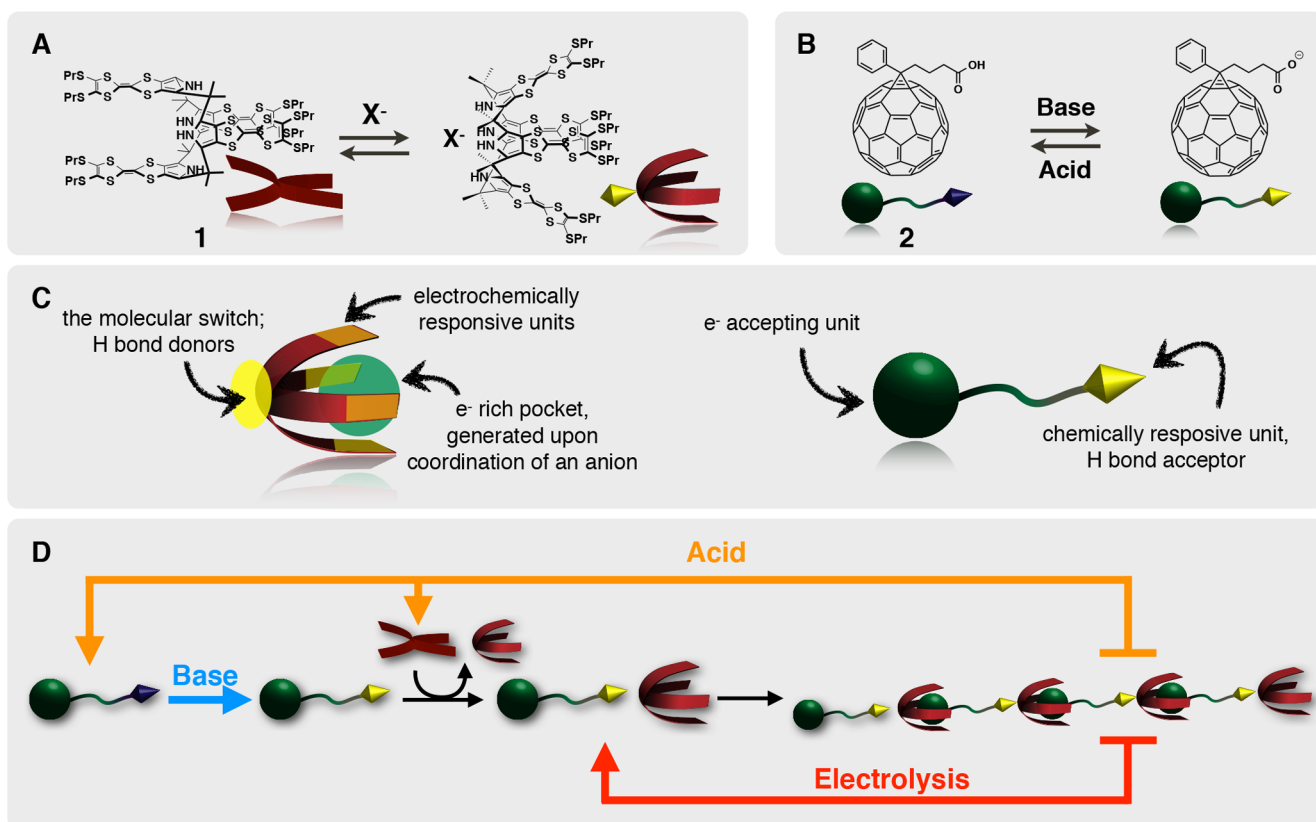


Figure 1. (A and B) Chemical structures of the heteroditopic monomers **1** and **2** used in this study and the underlying molecular design concept. (C) Illustrations of an anion-bound form of the thiopropyl-functionalized, tetrathiafulvalene-annulated calix[4]pyrrole (SPr-TTF-C[4]P **1**) and the phenyl C₆₁ butyric acid (PCBA **2**). (D) Schematic representation of the self-assembled structure produced from the cone conformer of **1** and the deprotonated form of **2**. Also shown is how this system may be controlled through acid–base chemistry and electrochemical oxidation.

the hydrolysis product of PCBM, an electron acceptor that has been extensively studied in the context of solar cell devices. The presence of a carboxylic acid group linked to a fullerene molecule was expected to allow several orthogonal interactions to be exploited for supramolecular assembly, including hydrogen-bonding and CT interactions. Moreover, the ability to deprotonate the carboxylic acid moiety was expected to allow self-assembly to be initiated via anion binding-induced conversion of the TTF-C[4]P subunit to the active cone conformation. The redox reactive nature of both the TTF and fullerene subunits was further expected to allow another level of control. A schematic representation of this design chemistry and the molecular structures of **1** and **2** are provided in Figure 1.

RESULTS AND DISCUSSION

As an initial test of whether **1** and **2** would undergo deprotonation-induced self-assembly, ¹H NMR spectroscopic studies were carried out wherein 1,8-diazabicyclo[5.4.0]undec-7-ene (DBU) was added to an equimolar solution of **1** and **2** in a 7:3 (v/v) mixture of CDCl₃ and CS₂ (Figure 2).²⁶ (Note: This solvent system, chosen for reasons of solubility, was used for all solution-phase analyses unless otherwise stated.) This addition led to several changes in the spectrum of compound **1**. For instance, the NH protons signal, originally at ca. 9.5 ppm, shifts to 11 ppm upon the addition of 1.4 equiv of DBU (Figures 2A and S1). A DBU-dependent broadening and splitting of the α proton signal of the thiopropyl substituents was also observed (Figure 2B). Such changes are rationalized in

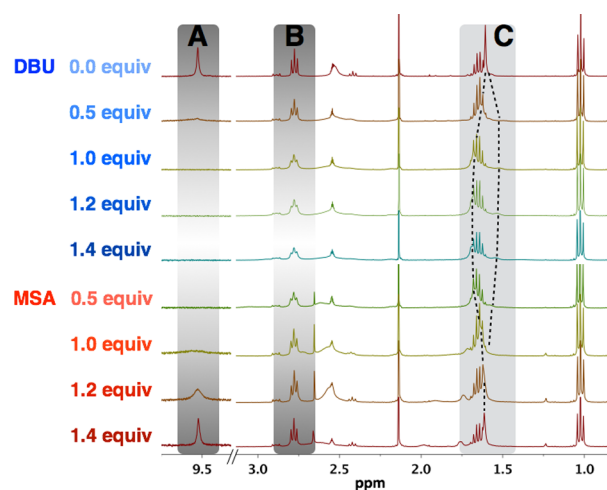


Figure 2. Partial ¹H NMR spectra recorded in a 7:3 mixture of CDCl₃ and CS₂ upon the sequential addition of DBU and MSA to an equimolar mixture of **1** and **2** (1 mM each). Highlighted are the signals for the (A) pyrrolic NH protons, (B) the α-protons of the thiopropyl substituents, and (C) the *meso*-methyl protons.

terms of the previously reported X-ray single crystal structure of the fullerene complex of **1**, wherein the bound substrate interacts closely with the α carbon of the thiopropyl groups.²³ Finally, changes in the *meso*-methyl proton signals were seen (Figure 2C). In the absence of a coordinating anion, the eight *meso*-methyl protons appear as a sharp, well-resolved singlet in the ¹H NMR spectrum, indicative of a species with time-

averaged D_{2d} point group symmetry. In sharp contrast, in the presence of a coordinating anion, **1** adopts a cone conformation with C_4 symmetry. As a result, the ^1H NMR signals of the *meso*-methyl groups are no longer magnetically equivalent, and two peaks are observed (Figure 2C). Upon the addition of methanesulfonic acid (MSA), all the DBU-induced spectral changes are reversed (*vide infra*).

2D ^1H ROESY NMR experiments provided evidence of an “on” and then “off” through-space proton coupling between **1** and **2** upon the sequential addition of base and acid in the 7:3 mixture of CDCl_3 and CS_2 (Figure S2).

CT interactions are thought to contribute to the interaction between the anion-bound form of **1** and the deprotonated form of **2** (the anion source). For instance, an increase in absorbance intensity in the 600–800 nm spectral region is seen upon addition of **1** to $(\mathbf{2} + \text{DBU})$ (Figure 3A). This intensity increase

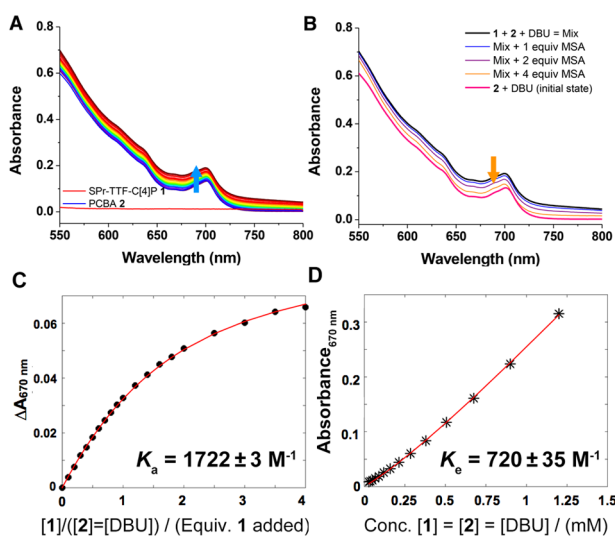


Figure 3. (A) UV–vis spectral changes seen upon the addition of **1** to an equimolar mixture of **2** and DBU ($[\mathbf{2}] = [\text{DBU}] = 0.5 \text{ mM}$). (B) Absorption changes seen upon addition of MSA. (C) Representative binding isotherm (670 nm) from the titration data in (A) showing the raw (black dots) and fitted data (red line) based on a simple 1:1 binding model. The resulting binding constant (K_a) for the interaction of **1** with $\mathbf{2} + \text{DBU}$ is also shown. (D) A representative binding isotherm (670 nm) from a dilution study (see Supporting Information) involving an equimolar mixture of **1**, **2**, and DBU ($[\mathbf{1}] = [\mathbf{2}] = [\text{DBU}]$) showing the raw data (black stars), fitted points (red line), and aggregation constant (K_e) obtained using the Hamelin–Jullien model²⁷ for the association and aggregation of two species.

was reversed upon adding acid (MSA) to the mixture (Figure 3B). The increase in absorptivity at longer wavelengths is consistent with a CT interaction between the TTF subunits and the bound fullerene moiety. Unfortunately, in contrast to what is true for pristine C_{60} , PCBA itself gives rise to a strong absorption band in this region. Thus, a clearly identifiable CT band could not be discerned. However, when ΔA at 670 nm (where **1** has essentially no absorptivity) is plotted as a function of $[\mathbf{1}]$, hyperbolic saturation behavior is seen (Figure 3C).

The association constant (K_a) for the binding of $(\mathbf{2} + \text{DBU}) + \mathbf{1}$ and the aggregation or equilibrium constant (K_e) for the aggregation of the complex $(\mathbf{2} + \text{DBU}) \cdot \mathbf{1}$ were estimated as $K_a = 1720 \text{ M}^{-1}$ (Figure 3C) and $K_e = 720 \text{ M}^{-1}$ (Figure 3D) from fitting of the titration data in Figure 3A and by performing a dilution study on an equimolar mixture of **1**, **2**, and DBU

(Figure S5), respectively (Figure 3). These binding constants were obtained by global nonlinear regression of the relevant UV–vis data between 550 and 800 nm based on an approach outlined by Hamelin and Jullien.²⁷ In their work, they consider the situation when a host H and a guest G can not only form a host–guest complex HG ($K_a = [\text{HG}]/[\text{H}][\text{G}]$), but also aggregate to form $(\text{HG})_n$ ($K_e = [\text{HG}]_n/[\text{HG}]^n$). This model may be applied with $\text{H} = (\mathbf{2} + \text{DBU})$, $\text{G} = \mathbf{1}$, and $(\mathbf{2} + \text{DBU}) \cdot \mathbf{1}$ as the aggregate precursors.

Hamelin and Jullien²⁷ point out that even though HG does aggregate ($K_e \neq 0$), aggregation may have little or no effect on spectral changes observed when H is titrated with G. The resulting data may then be fitted to a simple 1:1 model to obtain an apparent association constant $K_{\text{app}} = [\text{HG}]_{\text{app}}/[\text{H}][\text{G}]$ (where $[\text{HG}]_{\text{app}}$ is the apparent concentration of HG), as long as the total concentration of the host ($[\text{H}]_0$) is low or K_e is comparable or smaller than K_a (making the assumption $K_{\text{app}} \approx K_a$ justifiable). On the other hand, when an equimolar mixture of H and G is subject to serial dilution, aggregation would generally manifest itself more readily if $K_e \neq 0$. The concentration of free host ($[\text{H}]$) can then be obtained from a quintic (fifth-order) equation as a function of K_a , K_e , and $[\text{H}]_0$, a treatment known as the Hamelin–Jullien model.

In studying the aggregation of **1** and **2**, the titration data (Figure 3A) for the addition of **1** to $(\mathbf{2} + \text{DBU})$ were fitted to a simple 1:1 binding model²⁸ to obtain $K_{\text{app}} = K_a$ (since $K_e < K_a$; *vide infra*). A dilution study on an equimolar mixture of **1**, **2**, and DBU was then performed, and the results analyzed using the Hamelin–Jullien model. This allowed K_e to be derived by fixing K_a to the K_{app} value obtained from the 1:1 modeling of the titration data. The degree of polymerization (DPN) can also be estimated based on the calculated $[\text{H}]$ values and the Carothers equation with $\text{DPN} = [\text{H}]_0/[\text{H}]$ (see Supporting Information for all calculation details). At the highest concentration used in the dilution study, the DPN is estimated to be ≈ 2.5 with the DPN rising to ≈ 14 when $[(\mathbf{2} + \text{DBU}) \cdot \mathbf{1}] = 10 \text{ mM}$ (Figure S5).

More direct support for the formation of a self-assembled oligomeric ensemble came from a series of dynamic light scattering (DLS) experiments in *o*-dichlorobenzene solution. Specifically, we examined samples of $\mathbf{2} + \text{DBU}$, $[\mathbf{2} + \text{DBU}] + \mathbf{1}$, $[\mathbf{2} + \text{DBU} + \mathbf{1}] + \text{MSA}$ (Figure 4A and Table S1). We also carried out a series of measurements wherein equimolar

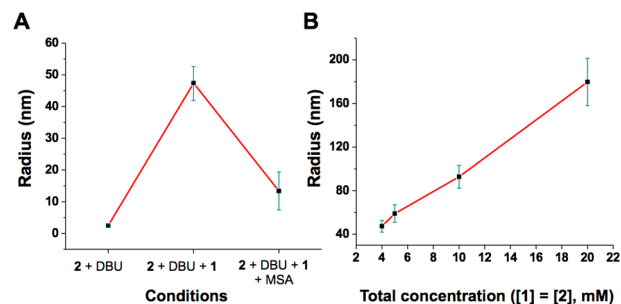


Figure 4. Summary of DLS studies. (A) Change in average radii of the self-assembled oligomers formed upon the addition of first **1** and then MSA to a solution of **2** in *o*-dichlorobenzene solution at 25 °C. The concentrations of **1** and **2** were 2 mM in these experiments. (B) Change in average radius reflecting the concentration-dependent behavior of the self-assembled oligomers formed from equimolar solutions of **1** and **2** in the presence of 3 molar equiv of DBU in *o*-dichlorobenzene solution at 25 °C.

mixtures of **1** and **2** were studied at varying total concentrations, namely 20, 10, 5, and 4 mM, in *o*-dichlorobenzene solution (Figure 4B and Table S2). As **1** is added to the mixture of **2** and DBU, the mean radii of oligomers in question increase up to 52 nm when the total monomer concentration is 4 mM ($[1] = [2] = 2$ mM). Adding MSA gives rise to oligomers with smaller mean radii, a finding that is fully consistent with the proposed breakup of the oligomeric assembly. Larger oligomers are seen as the total concentration of 1:1 mixtures of **1** and **2** in the presence of 3 equiv of DBU is increased. The largest effective mean radius for the oligomer, 198 nm, was recorded, as expected at the highest tested concentration ($[1] = [2] = 10$ mM).

¹H DOSY NMR studies were also carried out in *o*-dichlorobenzene. A direct correlation was found between the mean values of the diffusion coefficients recorded for the phenyl protons of **2** and the total concentration of 1:1 mixtures of **1** + **2** in the presence of 3 molar equiv of DBU. As expected for the formation of aggregates, the diffusion coefficient decreased as the net concentration of **1** + **2** increased (cf. Figure S4).

Taken in concert, the above findings provide critical experimental support for the formation of oligomers and their reversible nature.

We were keen to explore whether other input parameters could be used to modulate the assembly and disassembly process. In general, TTF-containing moieties undergo reversible oxidation from the neutral TTF to first the corresponding radical cation (TTF^{•+}) and then the dication (TTF²⁺).²⁹ These oxidized forms were expected to have a lower affinity for the fullerene. Oxidation of SP_r-TTF-C[4]P **1** was thus expected to engender release of the bound fullerene, inducing disassembly of the self-associated, oligomeric complex $[(2 + \text{DBU}) \cdot 1]_n$.

As a first step toward testing the above hypothesis, electrochemical studies were carried out. It was found that upon addition of DBU to a mixture of **1** (0.5 mM) and **2** (0.5 mM) in a 7:3 (v/v) mixture of CHCl₃ and CS₂, a positive shift in the TTF oxidation potential is seen in the cyclic voltammograms. Such a finding is easily rationalized in terms of a fullerene moiety being bound within the pocket of the calix[4]pyrrole.³⁰ Upon treatment with MSA, the original redox potential was restored (Figure 5). Again, such findings are consistent with the formation and subsequent break up of an oligomeric species, as shown in Figure 1D.

To test whether the self-assembled structures formed from **1** and 2·DBU might undergo depolymerization by means of a

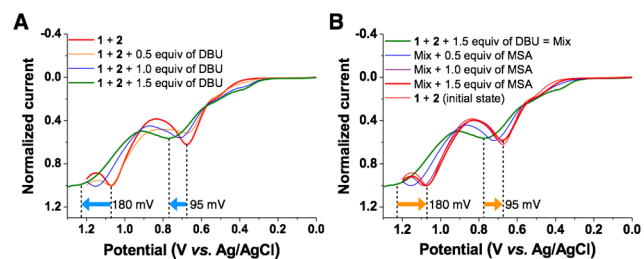


Figure 5. Linear sweep voltammograms of a mixture of **1** and **2** recorded upon the sequential addition of (A) DBU and (B) MSA. Measurements were performed using a Pt counter electrode, a Ag/AgCl reference electrode, and a glassy carbon working electrode in a 7:3 mixture of CHCl₃ and CS₂ containing THABF₄ (0.1 M) as the supporting electrolyte.

purely electrochemical stimulus (i.e., in the absence of reprotonation effects), it proved important to find electrolysis conditions wherein the four TTF arms of **1** are fully oxidized to their corresponding dicationic forms, without decomposition of media. Calculating the number of electrons in the CV curves was thus considered to be an important predicate. With such a view in mind, chronoamperometry experiments were first performed (under conditions that *D* is determined independent of solution concentration; see Supporting Information) so as to calculate the diffusion coefficients (*D*) of **1** and one of TTF arms **3** (Figure S6). Using the calculated *D*, the number of electrons at each oxidation current peak and potential could be obtained by³¹

$$i_{ss} = 4nFCDa$$

where i_{ss} is steady-state current attained at the tip, *n* is the number of electrons in the electrode reaction at the tip, *F* is the Faraday constant, *a* is the tip radius, and *C* and *D* are the concentration and diffusion coefficients of the solution species (Figure S6).

On the basis of the experiments shown in Figure 6, it was concluded that 1.6 V (vs Ag/AgCl) was the optimal potential

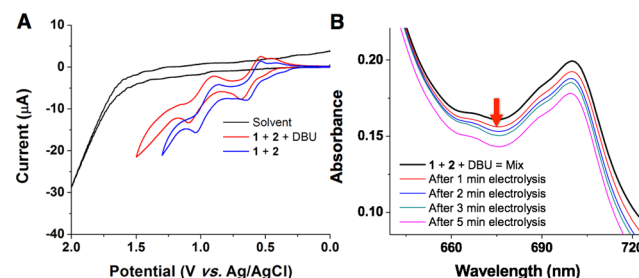


Figure 6. (A) Cyclic voltammograms of the solvent (black), a mixture of **1** and **2** containing DBU (red), and the same mixture without DBU (blue). (B) UV-vis spectroelectrochemistry of a 7:3 (v/v) CHCl₃:CS₂ solution containing **1** + **2** + DBU. Measurements were performed with a Pt counter electrode, a Ag/AgCl reference electrode, and a Pt mesh working electrode in the presence of THABF₄ (0.1 M) as a supporting electrolyte.

for achieving electrochemical switching without inducing electrolysis of the solvent (Figure 6A).^{32–35} Electrolysis of a mixture of **1**, **2**, and DBU at this potential was expected to allow the TTF subunits to be oxidized to their corresponding dicationic states. The mixture was thus electrolyzed at 1.6 V for 5 min using the single potential time base technique and subject to UV-vis spectroscopic analysis (Figure 6B). The absorbance decreases as the electrolysis proceeds. Such a finding provides support for the design contention that upon oxidation of TTF to its dicationic TTF²⁺ state, the TTF-containing host **1** loses its ability to bind well the electron-poor fullerene moiety (2·DBU). Breakup of the oligomers thus occurs. Thin-layer chromatographic and mass spectrometric analyses provide evidence that even after an electrolysis time of 40 min both **1** and **2** are released without evidence of appreciable decomposition being observed. However, we appreciate that failure to obtain evidence of decomposition under the conditions of such bulk electrolysis does not serve to rule out its occurrence at or near the electrode surface. Moreover, it is also important to stress that the electrochemical switching is of a one-way nature. We were unable to find electrochemical conditions that would

allow for cycling between the aggregated and disaggregated states.

CONCLUSIONS

Two chemical and redox responsive monomers were used to construct a supramolecular oligomeric material. The resulting ensemble could be modulated by means of chemical and electrochemical stimuli. The highly orthogonal nature of the control techniques detailed here is expected to aid in the design of stimulus-responsive systems where external factors are used to modulate structure and function over a range of length scales.

ASSOCIATED CONTENT

Supporting Information

The Supporting Information is available free of charge on the ACS Publications website at DOI: 10.1021/jacs.5b06524.

2D ^1H ROESY and DOSY NMR spectroscopic analyses; tables of errors for the DOSY NMR experiments; details of binding studies and electrochemical analyses; and results of DLS experiments (PDF)

AUTHOR INFORMATION

Corresponding Authors

*jinho_echem@sunghsin.ac.kr

*p.thordarson@unsw.edu.au

*sessler@cm.utexas.edu

Notes

The authors declare no competing financial interest.

ACKNOWLEDGMENTS

Support from the U.S. National Science Foundation (CHE-1402004 to J.L.S.), the Robert A. Welch Foundation (Grant F-1018 to J.L.S.), and the Australian Research Council (Future Fellowship FT120100101 to P.T.) is gratefully acknowledged. Thanks are also expressed to Lauren M. Strawsine for carrying out confirmatory electrolysis studies.

REFERENCES

- (1) Lewis, J. E. M.; Gavey, E. L.; Cameron, S. A.; Crowley, J. D. *Chem. Sci.* **2012**, *3*, 778–784.
- (2) Xuan, W.; Zhu, C.; Liu, Y.; Cui, Y. *Chem. Soc. Rev.* **2012**, *41*, 1677–1695.
- (3) Li, X.; Li, J.; Gao, Y.; Kuang, Y.; Shi, J.; Xu, B. *J. Am. Chem. Soc.* **2010**, *132*, 17707–17709.
- (4) Dankers, P. Y. W.; Harmsen, M. C.; Brouwer, L. A.; Van Luyn, M. J. A.; Meijer, E. W. *Nat. Mater.* **2005**, *4*, 568–574.
- (5) Stuart, M. A. C.; Huck, W. T. S.; Genzer, J.; Muller, M.; Ober, C.; Stamm, M.; Sukhorukov, G. B.; Szleifer, I.; Tsukruk, V. V.; Urban, M.; Winnik, F.; Zauscher, S.; Luzinov, I.; Minko, S. *Nat. Mater.* **2010**, *9*, 101–113.
- (6) Burattini, S.; Greenland, B. W.; Chappell, D.; Colquhoun, H. M.; Hayes, W. *Chem. Soc. Rev.* **2010**, *39*, 1973–1985.
- (7) Burnworth, M.; Tang, L.; Kumpfer, J. R.; Duncan, A. J.; Beyer, F. L.; Fiore, G. L.; Rowan, S. J.; Weder, C. *Nature* **2011**, *472*, 334–337.
- (8) Ge, Z.; Hu, J.; Huang, F.; Liu, S. *Angew. Chem., Int. Ed.* **2009**, *48*, 1798–1802.
- (9) Fenske, T.; Korth, H. – G.; Mohr, A.; Schmuck, C. *Chem. - Eur. J.* **2012**, *18*, 738–755.
- (10) Xu, J. – F.; Chen, Y. – Z.; Wu, D.; Wu, L. – Z.; Tung, C. – H.; Yang, Q. – Z. *Angew. Chem., Int. Ed.* **2013**, *52*, 9738–9742.
- (11) Dong, S.; Gao, L.; Li, J.; Xu, D.; Zhou, Q. *Polym. Chem.* **2013**, *4*, 3968–3973.

(12) Arotçaréna, M.; Heise, B.; Ishaya, S.; Laschewsky, A. *J. Am. Chem. Soc.* **2002**, *124*, 3787–3793.

(13) Jones, D. M.; Smith, J. R.; Huck, W. T.; Alexander, C. *Adv. Mater.* **2002**, *14*, 1130–1133.

(14) Verdejo, B.; Rodríguez-Llansola, F.; Escuder, B.; Miravet, J. F.; Ballester, P. *Chem. Commun.* **2011**, *47*, 2017–2019.

(15) Rodríguez-Hernández, J.; Lecommandoux, S. *J. Am. Chem. Soc.* **2005**, *127*, 2026–2027.

(16) Kim, D. S.; Lynch, V. M.; Park, J. S.; Sessler, J. S. *J. Am. Chem. Soc.* **2013**, *135*, 14889–14894.

(17) Park, J. S.; Yoon, K. Y.; Kim, D. S.; Lynch, V. M.; Bielawski, C. W.; Johnston, K. P.; Sessler, J. L. *Proc. Natl. Acad. Sci. U. S. A.* **2011**, *108*, 20913–20917.

(18) Kim, D. S.; Sessler, J. L. *Chem. Soc. Rev.* **2015**, *44*, 532–546.

(19) Wong, C. – H.; Zimmerman, S. C. *Chem. Commun.* **2013**, *49*, 1679–1695.

(20) Hu, X. – Y.; Xiao, T.; Lin, C.; Huang, F.; Wang, L. *Acc. Chem. Res.* **2014**, *47*, 2041–2051.

(21) Elacqua, E.; Lye, D. S.; Weck, M. *Acc. Chem. Res.* **2014**, *47*, 2405–2416.

(22) Hummelen, J. C.; Knight, B. W.; LePeq, F.; Wudl, F.; Yao, J.; Wilkins, C. L. *J. Org. Chem.* **1995**, *60*, 532–538.

(23) Fukuzumi, S.; Ohkubo, K.; Kawashima, Y.; Kim, D. S.; Park, J. S.; Jana, A.; Lynch, V. M.; Kim, D.; Sessler, J. L. *J. Am. Chem. Soc.* **2011**, *133*, 15938–15941.

(24) Davis, C. M.; Lim, J. M.; Larsen, K. R.; Kim, D. S.; Sung, Y. M.; Lyons, D. M.; Lynch, V. M.; Nielsen, K. A.; Jeppesen, J. O.; Kim, D.; Park, J. S.; Sessler, J. L. *J. Am. Chem. Soc.* **2014**, *136*, 10410–10417.

(25) Gale, P. A.; Sessler, J. L.; Král, V.; Lynch, V. M.; Lynch, J. M. *Chem. Soc.* **1996**, *118*, 5140–5141.

(26) Unless otherwise indicated, all measurements were performed in a mixture of $\text{CH}(\text{D})\text{Cl}_3:\text{CS}_2$ (7:3, v/v) containing a trace of $\text{DMSO}-d_6$. This was done for reasons of solubility.

(27) Hamelin, B.; Jullien, L. *J. Chem. Soc., Faraday Trans.* **1997**, *93*, 2153–2160.

(28) (a) Thordarson, P. *Chem. Soc. Rev.* **2011**, *40*, 1305–1323. (b) www.supramolecular.org (accessed June 17, 2015).

(29) Nielsen, M. B.; Lomholt, C.; Becher, J. *Chem. Soc. Rev.* **2000**, *29*, 153–164.

(30) Aprahamian, I.; Dichtel, W. R.; Ikeda, T.; Heath, J. R.; Stoddart, J. F. *Org. Lett.* **2007**, *9*, 1287–1290.

(31) Bard, A. J.; Fan, F. – R. R.; Kwak, J.; Lev, O. *Anal. Chem.* **1989**, *61*, 132–138.

(32) Applying a potential lower than 1 V (vs Ag/AgCl) leads to formation of the TTF radical cation (cf. ref 33).

(33) Bryce, M. R. *Adv. Mater.* **1999**, *11*, 11–23.

(34) Goldenberg, L. M.; Becker, J. Y.; Levi, O. P. – T.; Khodorkovsky, V. Y.; Shapiro, L. M.; Bryce, M. R.; Cresswell, J. P.; Petty, M. C. *J. Mater. Chem.* **1997**, *7*, 901–907.

(35) Torrance, J.; Scott, B.; Welber, B.; Kaufman, F.; Seiden, P. *Phys. Rev. B: Condens. Matter Mater. Phys.* **1979**, *19*, 730–741.